FLOW AND HEAT TRANSFER PERFORMANCE OF PLATE PHASE CHANGE ENERGY STORAGE HEAT EXCHANGER

by

Ji-Min ZHANG, Shi-Ting RUAN, Jian-Guang CAO*, and Tao XU

Shanghai Institute of Satellite Engineering, Shanghai, China

Original scientific paper
https://doi.org/10.2298/TSCI170821072Z

In the present work, the phase change energy storage heat exchanger in thermal control system of short-time and periodic working satellite payloads is taken as the research object. Under the condition of constant heated power of the satellite payload, the heat transfer characteristics of phase change energy storage heat exchanger are analyzed by numerical simulation and experimental method. The heat exchanger with fin arrays to enhance heat transfer is filled with tetradecane, whose density varies with temperature. The flow field distribution, the solid-liquid distribution, the temperature distribution, and the phase change process in the plate phase change energy storage heat exchanger unit are analyzed. The flow and heat transfer characteristics of heat exchangers under different fluid-flow rates and temperature were investigated.

Key words: *thermal control system, phase change energy storage, heat exchanger, fin arrays, phase change process*

Introduction

With the development in space technology, more and more special payloads with high-power and short-time periodic working characteristics, such as lasers and SAR antennas, have recently been used in satellites [1]. At present stage, fluid circuit and intermediate phase change energy storage technology are used to solve such a satellite payloads thermal control problem. When the satellite payload is working, the internal fluid circuit absorbs the heat of the satellite payload and stores the heat in the phase change energy storage heat exchanger and when the load is not working, the heat stored in the phase change energy storage heat exchanger is slowly drained through the small-scale external circuit [2].

As phase change material (PCM), paraffin has a wide range of phase change point, phase change latent heat and many other advantages, so it has a good application prospect in the field of spacecraft thermal control [3]. At present, the main factor restricting the development of paraffin is that its thermal conductivity is too small. Due to the low thermal conductivity of paraffin, heat is gathered in the paraffin near the heating surface. Paraffin near the heating surface melts first, resulting in volume expansion and phase change energy storage device burst and damage [4].

The technical means to improve the heat transfer performance of phase change devices mainly include: enhancing the thermal conductivity of PCM and Enhancing the heat transfer characteristics of heat transfer equipment. Some scholars [5, 6] studied the effect of the thermal conductive filler such as nanoparticle and expanded graphite on the thermal conductivity and thermal storage properties of PCM. Other scholars [7, 8] add metal materials to PCM, including

*Corresponding author, e-mail: ruan_shiting@163.com

metal chips, metal sheet, metal mesh and metal ball, and study the impact on the thermal conductivity of PCM. Ren *et al*. [9, 10] use fireworks algorithm and other intelligent algorithms to retrieve the physical parameters and optical parameters of PCM. In addition, some scholars [11-13] are dedicated to studying the effect of fin structures on thermal conductivity of PCM. The results show that the fins enhance the heat transfer by increasing the thermal conductivity and enhancing the natural convection. On the basis of the previous researches, the heat transfer performance of plate phase change energy storage heat exchanger with fin structures to enhance heat transfer was studied by numerical simulation and experimental method.

Numerical study

Physical model

A thermal control system of short, periodic working satellite payload is shown in fig. 1. When the satellite payload is working, the internal fluid circuit driven by the large flow pump absorbs the heat released by the satellite payloads and stores it in the phase change energy storage heat exchanger. When the satellite payload is not working, the external circuit driven by the small flow pump absorbs the heat in the phase change energy storage heat exchanger and slowly disperses the heat through a small scale radiator. The flow of the internal fluid circuit driven by the large flow pump and the state change of the phase change energy storage heat exchanger are studied when the satellite payload is working, ignoring the effect of external circuit on thermal control device.

The phase change energy storage heat exchanger is consist of 20 layers of PCM, 17 layers of internal fluid circuit, and 2 layers of external fluid circuit. The mass of PCM added into phase change energy storage heat exchanger is 1.49 kg, and there are 2136 fins in each layer. The size of fins is designed according to two reasons, one is machining ability, and another one is the loading capacity of heat exchanger. The round fins are obtained by reducing the drag of the cooling medium. The amount of fins are got basing on the volume ratio between fins and PCM. The staggered arrangement of fins is selected to improve the uniformity of flow field and heat transfer.

The heating power of satellite payload is 3.2 kW when it is working. The flow rates of pump are 3 L/min, 4 L/min, and 5 L/min, respectively. It is assumed that the heat of the load is completely absorbed by the working fluid (water). So the temperature rise of the working fluid is 15.3 K,11.5 K, and 9.2 K, respectively. The specific parameters under different operating conditions are shown in tab. 1.

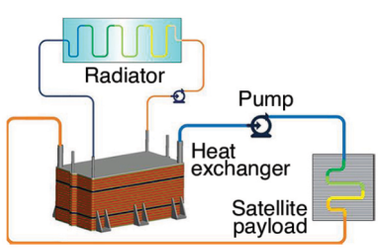

Figure 1. The thermal control system of the satellite payload

An internal circuit energy storage unit of phase change energy storage heat exchanger is considered to simulate the state change of PCM. Its physical model is shown in fig. 2. The internal circuit energy storage unit is composed of a fluid layer, a metal plate and the PCM. The fin arrays are arranged in the PCM to enhance heat conduction. The parameters of the unit size are shown in tab. 2.

Table 1. The specific parameters under different operating conditions Unit:K

Flow rate	Inlet temperature of the satellite payload	Outlet temperature of the satellite payload	Temperature rise	Inlet temperature of the heat exchanger	Initial temperature
3 l/min	277	292.3	15.3	292.3	277
4 l/min	277	288.5	11.5	288.5	277
5 l/min	277	286.2	9.2	286.2	277

In this work, tetradecane is used as PCM. A real paraffin blend, like tetradecane, does not have sharply defined *solidus* and *liquidus* temperatures, and its enthalpy is a continuous function of the temperature. In the present work, a melting interval of 278 K-279 K is used, as a first step from a *sharp* phase change analysis to a more realistic representation. Material density of the PCM depends on their temperature. Considering computational continuity during phase change, the density is calculated with the following relations:

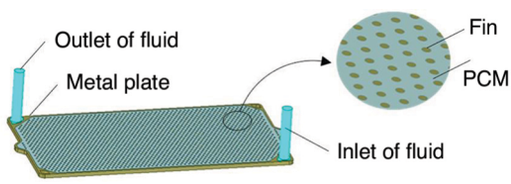

Figure 2. The internal circuit energy storage unit

$$\rho = \frac{762.8}{0.005\,(T - 278.5) + 1} \tag{1}$$

Table 2. The parameters of the internal circuit energy storage unit, Unit: mm

PCM $l \times w \times h$	Fin $d \times h$	Inlet and outlet $d \times h$	Fluid layer $l \times w \times h$	Metal plate $l \times w \times h$
246 × 126 × 3.5	1.5 × 3.5	10 × 40	246 × 126 × 1.2	250 × 130 × 0.4

Aluminum is used as the metal material. The detailed physical properties of tetradecane, water and aluminum are shown in tab. 3.

Table 3. The properties of the different materials

Materials	Density [Kgm^{-3}]	Thermal conductivity [$Wm^{-1}K^{-1}$]	Dynamic viscosity [$kgm^{-1}s^{-1}$]	Latent heat [$kJkg^{-1}$]	Melting point [K]
$C_{14}H_{30}$	eq.(1)	0.1499	0.00796	226	278-279
Al	2700	237	–	–	–
H_2O	1000	0.6	0.001003	–	–

Computational procedure

For the phase change region inside the PCM, enthalpy-porosity approach [14-16] is used, by which the porosity in each cell is set equal to the liquid fraction in that cell. Accordingly, the porosity is zero inside fully solid regions. It is worth to note here that Bertrand *et al*. [17] present the results of a comparison exercise in which various numerical approaches were applied to a phase change problem that included coupled natural convection and melting, covering two ranges of Prandtl numbers, which corresponded to the melting of metals and organic materials. The results indicate that enthalpy methods are to be used in most phase change problems where a solid-liquid interfacial region is present between the phases. During the simulation process, the solid-liquid interface is determined by the change of the liquid phase rate during the phase change process of PCM. The region where the liquid phase and the solid phase coexist is treated as porosity.

Therefore, the governing conservation equations used here for the PCM system are:

Continuity:

$$\frac{D\alpha_n}{Dt} = 0 \tag{2}$$

Momentum:

$$\rho\frac{D\vec{v}}{Dt} = -\nabla P + \mu\nabla^2\vec{v} + \rho\vec{g} + \vec{S} \tag{3}$$

Energy:

$$\rho\frac{D\tilde{h}}{Dt} = k\nabla^2 T \tag{4}$$

where α_n is the n^{th} fluid's volume fraction in the computational cell, ρ – the density, k – the thermal conductivity, μ – the dynamic viscosity, $\vec{S}$ – the momentum source term, $\vec{v}$ – the velocity component, and h – the specific enthalpy. The latter is defined as a sum of the sensible enthalpy:

$$\tilde{h}_s = \tilde{h}_{ref} + \int_{T_{ref}}^{T} c_p \mathrm{d}T \tag{5}$$

the enthalpy change due to the phase change γ_L, where h_{ref} is the reference enthalpy at the reference temperature T_{ref}, c_p – the specific heat, L – the specific enthalpy of melting (latent-heat of the material), and γ – the liquid fraction during the phase-change which occurs over a range of temperatures $T_s < T < T_l$, defined by the following relations:

$$\left.\begin{aligned} \gamma &= 0, (T < T_s) \\ \gamma &= \frac{T - T_s}{T_l - T_s}, (T_s < T < T_l) \\ \gamma &= 1, (T < T_l) \end{aligned}\right\} \tag{6}$$

the source term $\vec{S}$ in the momentum equation is given by $\vec{S} = -A(\gamma)\,\vec{v}$, where $A(\gamma)$ is the *porosity function* defined by Brent *et al*. [15]. Definition of $A(\gamma)$ makes the momentum equation *mimic* Carman-Kozeny equations for flow in porous media:

$$A(\gamma) = \frac{C\,(1-\gamma)^2}{\gamma^3 + \varepsilon} \tag{7}$$

where $\varepsilon = 0.001$ is a small computational constant used to avoid division by zero, and C is a constant reflecting the morphology of the melting front. This constant is a large number, usually 10^4-10^7. A value of $C = 10^5$ has been used in the previous study [18], where its effect was discussed. The same value of C is adopted herein.

The computational meshes are generated by ICEM, which is packaged with CFD software ANSYS. The computational domain is divided into three parts: the metal region, water region, and PCM region. The computation domain is discretized by nonuniform grids with more refined grids in the PCM region.

The accuracy of grid system has been carefully testified to keep under reasonable limits the computational time. Three grids size, 8, 10, and almost 12 millions cells, are used to verify grid independence. Finally, 8 millions cells had been chosen for the further work. The time step can be selected based on the Courant-Friedrichs-Lewy (CFL) condition as $\Delta t \leq \Delta x/v$ [19], where Δx is the characteristic dimension of the cell and v is the velocity. The value of Δt based on the CFL is 0.3 seconds, and the present work chosen 0.001 seconds as time-step in order to obtain the convergent result.

The commercial CFD software, FLUENT 14.5 based on the finite volume method is employed to account for the phase change process with additional user defined functions written in *C* language to describe the density of PCM. The convergence is checked at each time-step and convergence criterion are the scaled residuals less than 10^{-6} for the continuity equation, 10^{-6} for the momentum equation and 10^{-6} for the energy equation.

Experimental set-up and results

Experimental set-up

In the present study, the experiment is designed to meet the conditions explored in the numerical investigation to some extent. The experiment using tetradecane as the PCM, and the initial temperature is 277 K. The experiment includes the following two series: (1) $Q = 4$ l/min, $T = 292.3$ K; $Q = 4$ L/min, $T = 288.5$ K; $Q = 4$ L/min, $T = 286.2$ K and (2) $Q = 3$ L/min, $T = 288.5$ K; $Q = 4$ L/min, $T = 288.5$ K; $Q = 5$ l/min, $T = 288.5$ K.

Experimental set-up is shown in fig. 3, including the following parts: phase change energy storage heat exchanger with 1.49 kg tetradecane, low-constant temperature bath A, low-constant temperature bath B, pump A, pump B, thermometer, flowmeter. In the present work, the satellite payload is short-time periodic work, and the time it works is always about 100 seconds. When the work is finished, the satellite payload and heat exchanger have enough time to cool down. In the physical model, the initial temperature of water is 277 K, and temperature will be 288.5 K after it absorbed the heat from the payload (flow rate is 4 L/min). Then, the temperature of water will cool down to the initial temperature when the water passes through the heat exchanger in initial 100 seconds. So it is reasonable to replace the payload with a constant temperature bath.

Set the temperature of the low-constant temperature bath A and B in advance. At the initial moment, close the pump A, open the pump B, the cryogenic fluid in the low-constant temperature bath B flows into the phase change energy storage heat exchanger, so that the temperature of the heat exchanger reaches the initial temperature of 277 K. Then, close the pump B, open the pump A, so that the hydrothermal fluid in low-constant temperature bath A flow into the heat exchanger. By changing the pump a speed way to adjust the flow, the flow rate is adjusted by changing the pump's speed. The temperature of the outlet fluid of the energy storage heat exchanger is recorded by the thermometer.

In this experiment, the thermometer consists of Agilent 34970A data acquisition and T-type thermocouple, using two DC-4006 low-constant temperature baths which total heating power is 4 kW as the low-constant temperature bath A, using DC-1030 low-constant temperature bath as the low-constant temperature bath B, using LWGY-2 turbine flowmeter.

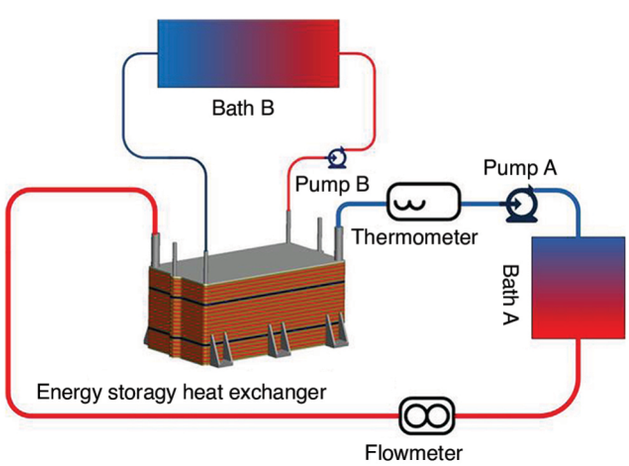

Figure 3. Experimental set-up

Validation of the numerical model

Figure 4 shows the comparison of the measured fluid temperature and simulated fluid temperature of the heat exchanger outlet *vs*. time for the case with flow rate of 4 l/min and the inlet temperature of the heat exchanger of 288.5 K. It can be seen from the figure that the measured fluid temperature of the heat exchanger outlet is higher than the numerical simulation results. The reason may be that the thermal resistance between metallic materials and PCM impedes heat transfer before PCM melts. What is more, the measured temperature of outlet fluid rises earlier but slower before it reached phase change point (288.5 K), it may be caused by two reasons. The first one is that the thermal resistance between metallic materials and PCM impedes heat transfer. Another one is that the heat is absorbed by latent heat while PCM melts. In general, the numerical simulation results are in agreement with the experimental results. Therefore, the numerical model can be used to predict the fluid flow and heat transfer performances of the phase change energy storage heat exchanger.

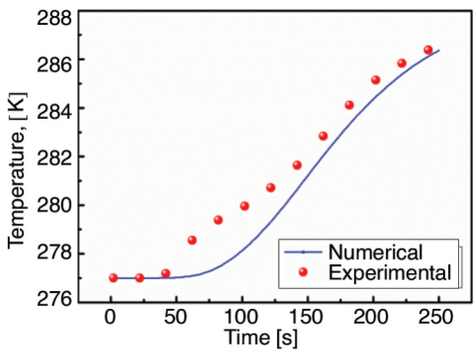

Figure 4. Comparison of the experimental results with the numerical simulation results

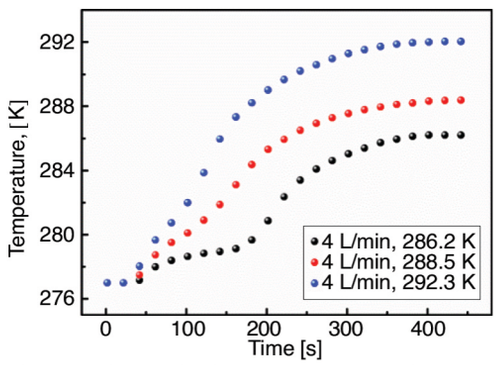

Figure 5. Outlet liquid temperature *vs.* time at fixed flow rate

Experimental results

In order to check how the value of some working parameter influences the heat transfer, the temperature of water in bath B is changed three times at the fixed flow rate, and the flow rate of pump A is changed three times too at the fixed temperature in the experiment. So, the experiments include the following two series: (1) Q = 4 L/min, T = 292.3 K; Q = 4 L/min, T = 288.5 K; Q = 4 L/min, T = 286.2 K; (2) Q = 3 l/min, T = 288.5 K; Q = 4 L/min, T = 288.5 K; Q = 5 L/min, T = 288.5 K. The results of experiments are showed in figs. 5 and 6.

As showed in fig. 5, when the temperature of water in bath B is changed at the fixed flow rate, there are obvious differences in different cases. When the outlet liquid temperature exceeds the phase change point (278.5 K), this temperature increases rapidly, especially in the case with flow rate of 3 L/min and the inlet temperature of the heat exchanger of 288.5 K. The reason may be that the thermal resistance between metallic materials and PCM impedes heat transfer before PCM melts, as previously mentioned. When the flow rate is changed at the fixed temperature of water in bath B, the differences among different cases are smaller. But they have the same phenomenon that the temperature of outlet fluid increases rapidly when it exceeds 278.5 K. In a word, the lower the temperature or the flow rate, the slower the temperature rise.

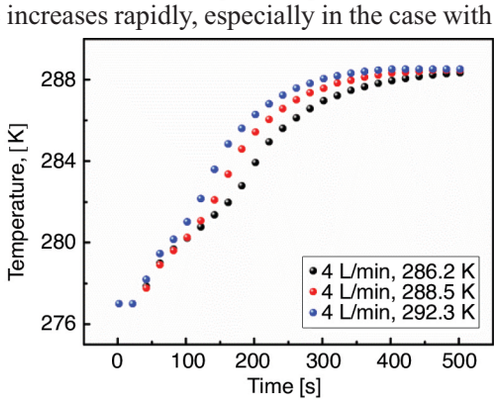

Figure 6. Outlet liquid temperature *vs.* time at fixed temperature of the water in bath B

Numerical simulation results and discussion

This section presents a detailed parametric study of melting, flow and heat transfer about the numerical simulation results. So, the numerical simulation includes the following three cases: (1) Q = 3 L/min, T = 292.3 K, (2) Q = 4 L/min, T = 288.5 K, and (3) Q = 5 L/min, T = 286.2 K.

The analysis of flow

The velocity distribution has the same rule at the different flow rates, and its distribution is shown in fig. 7. In the import and export area, the fluid speed is large. In the corner area on both sides of the import and export, the fluid velocity is small. This phenome-

non is detrimental to achieving uniform heat transfer. In the process of designing the heat exchanger, it can effectively improve the uniformity of the flow field by changing the fins distribution. In this paper, the flow field has been optimized by increasing the distance between fins and boundary. Compared with the unmodified plate heat exchanger, the flow velocity in the corner area on both sides of the import and export has been improved.

The analysis of phase change process

Although the heat transfer fluids carry the same heat, their impact on the phase change energy storage unit are different at different flow rates. It can be seen from fig. 8 that the melting time of PCM is the shortest when Q = 5 L/min and T = 286.2 K. And PCM melts complete at T = 150 seconds. The melting time of PCM is the longest when Q = 3 L/min and T = 292.3 K. And PCM melts complete at T = 210 seconds. The difference in melting time is caused by the difference in heat flux. However, it can be seen from fig. 8 that the heat flux is the same when T < 50 seconds, but the melting speed of the PCM is different. The main reason for this phenomenon is that the difference of sensible heat absorbed from the fluid to the PCM. The sensible heat absorbed by the PCM is higher, the latent heat is smaller when Q = 3 L/min and T = 292.3 K, so the melting speed is slower; the sensible heat absorbed by the PCM is lower, the latent heat is higher when Q = 5 L/min and T = 286.2 K, so the melting speed is larger.

As shown in fig. 8, the heat flux of the heat transfer fluid varies with time, and the rate of change varies in the three cases. The change in heat flux is determined by the amount of heat transfer between the heat transfer fluid and the PCM. The outlet fluid temperature of the heat exchanger rises first, resulting in a decrease first in the heat flux when Q = 5 L/min and T = 286.2 K. The outlet fluid temperature of the heat exchanger rises later, resulting in a decreases later in the heat flux when Q = 3 L/min and T = 292.3 K. And the change of outlet liquid temperature is synchronized with the change of heat flux.

The phase change process is analyzed when the flow rate is 3 L/min and the temperature is 292.3 K. The solid-liquid distribution is shown in fig. 9. At the beginning of the melting, the liquid state of the PCM distribution is fan-shaped along the inlet, as shown in fig. 9(a). With the passage of time, the fan-shaped area is slowly expanding, as shown in fig. 9(b), (c). Because the flow area is mainly concentrated on the import and export connection area, PCM

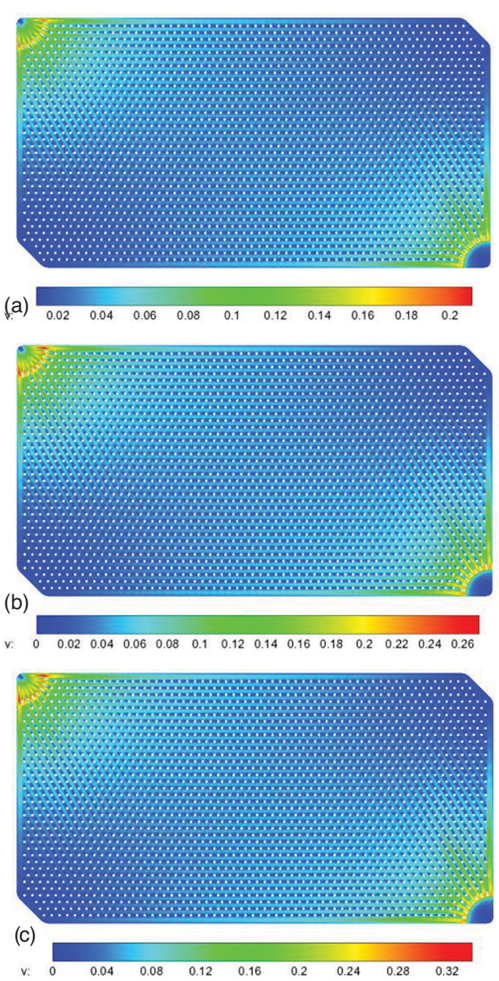

Figure 7. Velocity distribution for different cases; (a) Q = 3 L/min, T = 292.3 K, (b) Q = 4 L/min, T = 288.5 K, and (c) Q = 5 L/min, T = 286.2 K

melts firstly along the connection area, and PCM melts slowly in the corner area to the end of the melting, as shown in fig. 9(d). This phenomenon caused the nonuniformity of the PCM melting process, reducing the utilization efficiency of the PCM. In order to compare the effect of the different cases on the phase change process in more detail, the solid liquid distribution were compared at different cross sections under the different cases when the melt fraction is 0.6, as shown in fig. 10. In the figure, the cases are 3 L/min, 292.3 K, 4 L/min, 288.5 K and 5 L/min, 286.2 K from top to bottom respectively. It can be seen from the figure, the melting difference between the bottom and the top of the PCM is smaller in the case of low flow rate. The melting difference between the bottom and the top of the PCM is larger in the case of high flow rate. The bottom melting region is larger and the top melting zone is smaller at the flow rate of 5 L/min, as shown in fig. 10(c). The reason is that heat transfer area is wide when the flow rate is high, resulting in large heat transfer difference between the bottom and top heat; and heat transfer area is narrow when the flow rate is low, resulting in small heat transfer difference between the bottom and top heat.

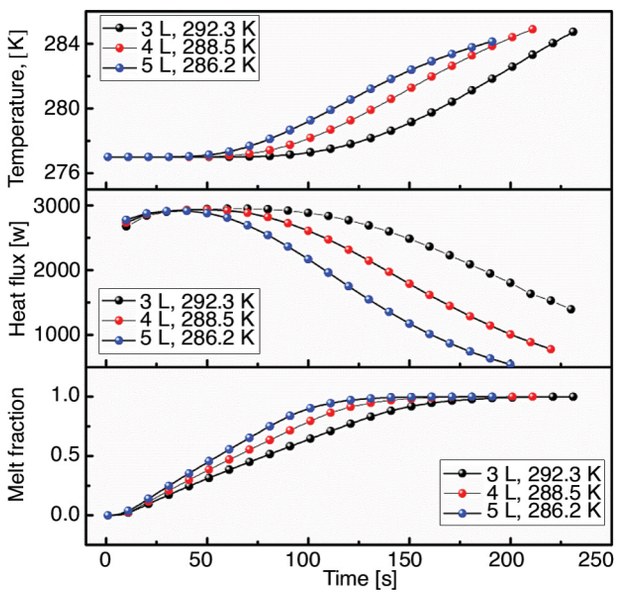

Figure 8. The change of melt fraction, heat flux, outlet liquid temperature *vs.* time

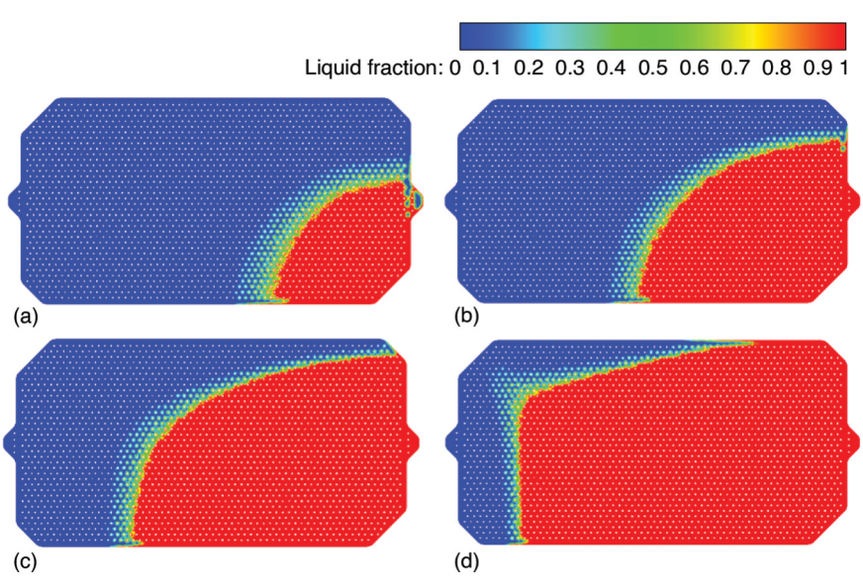

Figure 9. Solid-liquid distribution throughout the melting process; (a) ϕ = 0.2 (b) ϕ = 0.4, (c) ϕ = 0.6, and (d) = 0.8

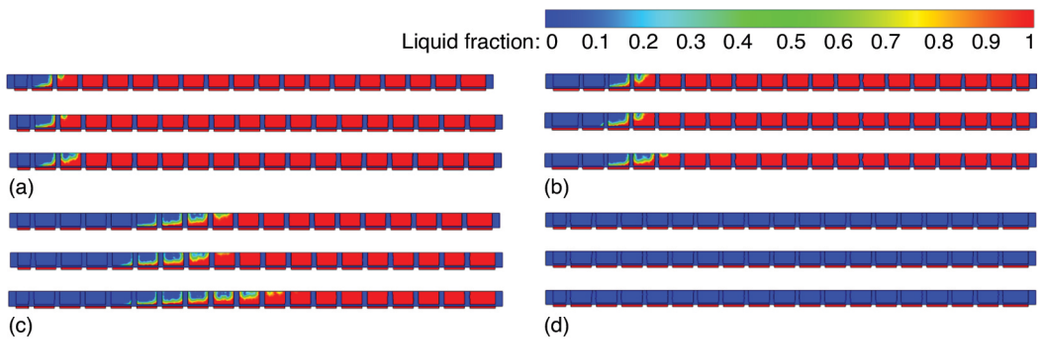

Figure 10. Temperature distribution of different cross-sections when the melt fraction is 0.6; (a) $l/l_0 = 0.2$, (b) $l/l_0 = 0.4$, (c) $l/l_0 = 0.6$, and (d) $l/l_0 = 0.8$

Different conditions have different effects on the outlet fluid temperature and temperature distribution of the energy storage heat exchanger. Figure 8 shows the change of outlet fluid temperature with time in different cases. With the passage of time, the outlet fluid temperature increased first at the flow rate of 5 L/min. As previously described, heat transfer area is wider when the flow rate is higher. So the outlet fluid temperature first increased.

The temperature distribution was analyzed during the melting process when the flow rate is 3 L/min and the inlet temperature is 292.3 K. The temperature distribution is shown in fig. 11. Its distribution is consistent with the solid-liquid distribution. Heat exchanger inlet fluid temperature first increased, and then developed along the streamline. As can be seen, the fin temperature is significantly higher than the surrounding PCM temperature. It can be concluded that the phenomenon of fins in enhancing heat transfer is very obvious. The cases are 3 L/min, 292.3 K, 4 L/min, 288.5 K and 5 L/min, 286.2 K from top to bottom, respectively.

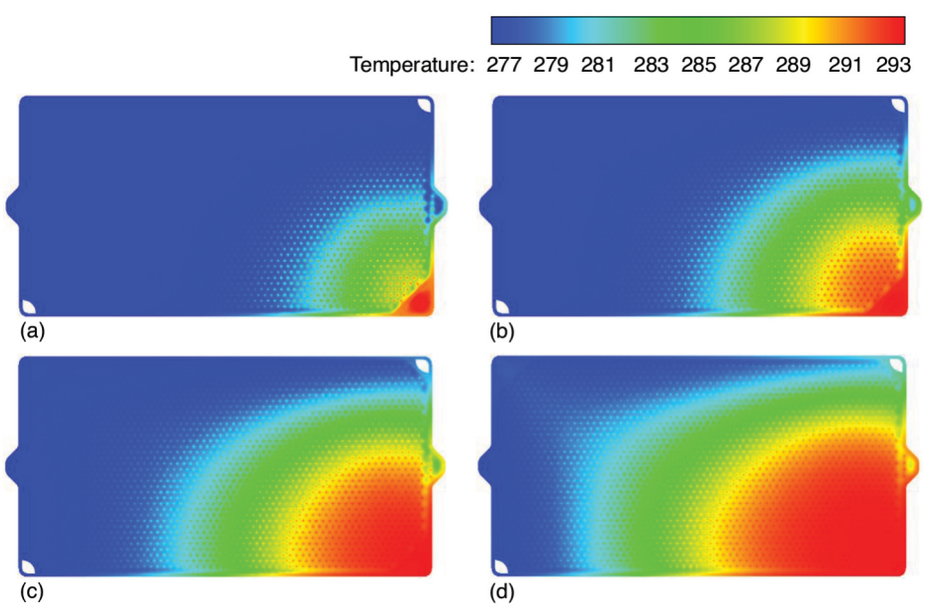

Figure 11. Temperature distribution for different cases; (a) $\phi = 0.2$, (b) $\phi = 0.4$, (c) $\phi = 0.6$, and (d) $\phi = 0.8$

Temperature distribution of different cross sections in phase change process was analyzed. Take the dimensionless temperature nonminmaxmin $T_{non} = (T - T_{min}) / (T_{max} - T_{min})$ as the reference temperature, and the temperature distribution shown in fig. 12. As shown from the figure, the temperature change is relatively large along the PCM height direction in the case of high flow rate. At the bottom of the PCM, the distribution of the high temperature is wider; at the top of the PCM, the distribution of the high temperature is narrower. In the case of low flow rate, the difference between the bottom and the top of the PCM is small. The main reason for this phenomenon is that the heat can be transfer to a larger area in the case of high flow rate, so the heat transfer along the height direction is relatively small.When the flow rate is low, the heat transfer area is limited, and then the heat transfer along the height direction is larger.

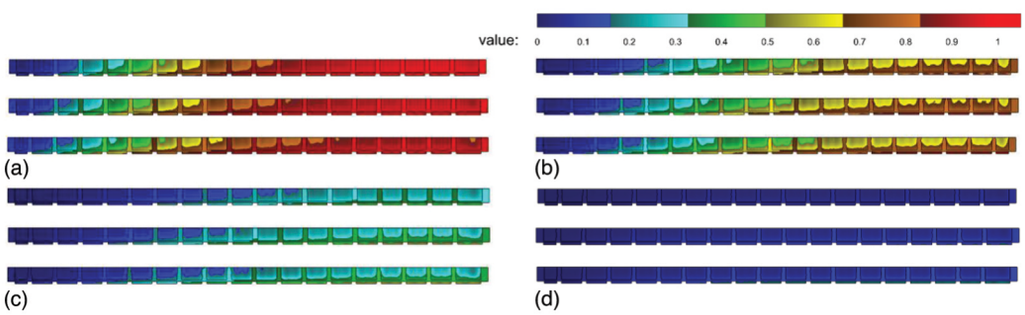

Figure 12. Temperature distribution of different cross sections when the melt fraction is 0.6; (a) $l/l_0 = 0.2$, (b) $l/l_0 = 0.4$, (c) $l/l_0 = 0.6$, and (d) $l/l_0 = 0.8$

Conclusions

In this paper, numerical and experimental simulation of plate phase change energy storage heat exchanger is carried out to study the energy storage performance of phase change energy storage heat exchanger with constant satellite payloads power. The flow field distribution, the solid-liquid distribution, and the temperature distribution of the heat exchanger were analyzed by using tetradecane as the PCM. The following conclusions were obtained.

- According to the results, this plate phase change energy storage heat exchanger has good heat dissipation ability for special payloads with high-power and short-time periodic working characteristics. When the payloads are short-time working, the internal fluid circuit can absorb the heat of the satellite payload and stores the heat in the phase change energy storage heat exchanger. And the maximum time of the short-time periodic working payloads is got according to the results. This result can be used to improve the thermal design of this kind of payloads.
- The velocity of the fluid in the inlet and outlet is large, and the flow velocity is small in the corner on both sides of the import and export. This phenomenon is detrimental to achieving uniform heat transfer. It can effectively improve the uniformity of the flow field by changing the fins distribution.
- In the same amount of heat absorption, when the flow rate is lower, the sensible heat absorbed by the PCM is higher, and the melting is slower. When the flow rate is high, the PCM absorbs less sensible heat and melts faster.
- The heat transfer amount from the fluid to the PCM is negatively correlated with the outlet fluid temperature of the heat exchanger. When the flow rate is slow, the temperature of the outlet fluid of the heat exchanger increases slowly and the amount of heat transfer remains constant for a long time.

- The heat can be transfer to a larger area in the case of high flow rate, so the heat transfer along the height direction is relatively small; when the flow rate is low, the heat transfer area is limited, and then the heat transfer along the height direction is more.

Nomenclature

A – porosity function, [–]
c_p – the specific heat, [Jkg^{-1}K^{-1}]
d – diameter, [mm]
h – height, [mm]
$\tilde{h}$ – enthalpy, [Jkg^{-1}]
k – conductivity, [Wm^{-1}K^{-1}]
L – latent heat, [kJkg^{-1}]
l – length, [mm]
l_0 – overall length, [mm]
Q – rate of flow, [Lmin^{-1}]
T – temperature, [K]
t – time, [s]
$\vec{v}$ – velocity, [ms^{-1}]
v – velocity, [ms^{-1}]

Greek symbols

α – phase volume fraction, [–]
γ – liquid fraction, [–]
ϕ – melt fraction, [–]
μ – dynamic viscosity, [kgm^{-1}s^{-1}]
ρ – density, [kgm^{-3}]

Subscripts

l – liquid
ref – reference value
s – solid

References

[1] Zhang, J., *et al.*, The Use of Fluid Loop on Large Spacecraft, *Proceedings*, 6th Space Thermal Physics Conference, Beijing, China, 2003
[2] Cheng, X., *et al*., Lightweight Design for Fluid Loops of Active Thermal Control System in Manned Spacecraft, *Manned Spacecraft*, *18* (2012), 4, pp. 30-35
[3] Theodore, D., *et al*., NASA Thermal Control Technologies for Robotic Spacecraft, *Apply Thermal Engineering*, *23* (2003), 9, pp. 1055-1065
[4] Leimkuehler, T. O., *et al*., Testing and Failure Mechanisms of Ice Phase Change Material Heat Exchangers, *Proceedings*, International Conference on Environmental Systems (ICES), Portland, Ore. USA, 2011
[5] Ranjbar, A. A., *et al*., Numerical Heat Transfer Studies of a Latent Heat Storage System Containing Nano-Enhanced Phase Change Material. *Thermal Science*, *15* (2011), 1, pp. 169-181
[6] Kashani, S., *et al*., Numerical Analysis of Melting of Anoenhanced Phase Change Material in Latent Heat Thermal Energy Storage System. *Thermal Science*, *18* (2014), 2, pp. 335-345
[7] Cabeza, L. F., *et al*., Heat Transfer Enhancement in Water When Used as PCM in Thermal Energy Storage, *Applied Thermal Engineering*, *22* (2002), 10, pp. 1141-1151
[8] Ettouney H. M., *et al*., Heat Transfer Enhancement by Metal Screens and Metal Spheres in Phase Change Energy Storage Systems, *Renewable Energy*, *29* (2004), 6, pp. 841-860
[9] Ren, Y. T., *et al*., Application of an Improved Firework Algorithm for Simultaneous Estimation of Temperature-Dependent Thermal and Optical Properties of Molten Salt, *International Communications in Heat and Mass Transfer*, *77* (2016), Oct., pp.33-42
[10] Ren, Y. T., *et al*., Simultaneous Retrieval of Temperature-Dependent Absorption Coefficient and Conductivity of Participating Media, *Scientific Reports*, *6* (2016), Feb., 21998
[11] Bugaje I. M., Enhancing the Thermal Response of Latent Heat Storage Systems, *Energy Research*, *21* (1997), 9, pp. 759-766
[12] Fol, S. C., Shen, W., Cooling of Portable Hand-Held Electronic Devices Using Phase Change Materials in Finned Heat Sinks, *International Journal of Thermal Sciences*, *49* (2010), 1, pp. 109-117
[13] Liu Z., *et al*., Experimental Investigations on the Characteristics of Melting Processes of Stearic Acid in an Annulus and its Thermal Conductivity Enhancement by Fins, *Energy Conversion and Management*, *46* (2005), 6, pp. 959-969
[14] Voller, V. R., *et al*., An Enthalpy Method for Convection/Diffusion Phase Change, *Int. J. Numer. Meth. Eng.*, *24* (2010), 1, pp. 271-284
[15] Brent, A. D., *et al*., Enthalpy-Porosity Technique for Modeling Convection-Diffusion Phase Change: Application to the Melting of a Pure Metal, *Numerical Heat Transfer*, *13* (1988), 3, pp. 297-318
[16] Voller, V. R., An Overview of Numerical Methods for Solving Phase Change Problems, *Advances in Numerical Heat Transfer*, *1* (Ed. W. Minkowycz), CRC Press, Bocu Raton, Fla., USA, 1996, Vol, 1, Chap. 6
[17] Bertrand, O., *et al*., Melting Driven by Natural Convection, A Comparison Exercise: First Results, *International Journal of Thermal Science*, *38* (1999), 1, pp. 5-26

[18] Shatikian,V., *et al*., Numerical Investigation of a PCM-Based Heat Sink With Internal Fins, *International Journal of Heat Mass Transfer, 48* (2005), 5-6, pp. 3689-3706
[19] Ye, W. B., *et al*., Fluid Flow and Heat Transfer in a Latent Thermal Energy Unit with Different Phase Change Material (PCM) Cavity Volume Fractions, *Applied Thermal Engineering, 42* (2012), 3, pp. 49-57

Paper submitted: August 21, 2017
Paper revised: November 7, 2017
Paper accepted: December 26, 2017